THE ASTROPHYSICAL JOURNAL, 425:622–634, 1994 April 20

STEPS TOWARD DETERMINATION OF THE SIZE AND STRUCTURE OF THE BROAD-LINE REGION IN ACTIVE GALACTIC NUCLEI. VII. VARIABILITY OF THE OPTICAL SPECTRUM OF NGC 5548 OVER 4 YEARS

B. M. PETERSON,[1] P. BERLIND,[2] R. BERTRAM,[1,3] N. G. BOCHKAREV,[4] D. BOND,[5] M. S. BROTHERTON,[6] J. R. BUSLER,[7] K. K. CHUVAEV,[8] R. D. COHEN,[9] M. DIETRICH,[10] M. ELVIS,[2] A. V. FILIPPENKO,[11] C. B. FOLTZ,[12] P. M. GARNAVICH,[5] L. C. HO,[11] E. HORINE,[2,13] K. HORNE,[14,15] J. P. HUCHRA,[2] W. KOLLATSCHNY,[10] K. T. KORISTA,[1,14,16] M. A. MALKAN,[17] T. MATHESON,[11] M. MIGNOLI,[18] S. L. MORRIS,[5,19] L. NAZAROVA,[20] J. PENFOLD,[7,21] J. PETERS,[2] R. W. POGGE,[1] V. I. PRONIK,[8] B. RUSH,[17] S. G. SERGEEV,[8] A. I. SHAPOVALOVA,[22] J. C. SHIELDS,[1,11,23] G. M. STIRPE,[18] S. TOKARZ,[2] R. M. WAGNER,[1,3] R. J. WEYMANN,[16] R. J. WHITE,[1,17] B. J. WILKES,[2] D. WILLS,[6] B. J. WILLS,[6] C. WINGE,[1,24] AND P. F. YOUNGER[5]

Received 1993 July 23; accepted 1993 October 25

ABSTRACT

We report on the results of a continuation of a large monitoring program of optical spectroscopy of the Seyfert 1 galaxy NGC 5548. The new observations presented here were obtained between 1990 December and 1992 October, and extend the existing database to nearly 1400 days, dating back to 1988 December. The continuum variations are generally smooth and well-resolved, except during the third year of this 4 year project, when the variations were apparently more rapid and of lower amplitude than observed at other times. The broad Hβ emission line is found to vary in response to the continuum variations with a lag of about 18 days, but with some changes from year to year. The Hβ transfer functions for each of the 4 yr and for the entire 4 yr database are derived by using a maximum entropy method.

Subject headings: galaxies: active — galaxies: individual (NGC 5548) — galaxies: nuclei — galaxies: Seyfert

1. INTRODUCTION

Intensive spectroscopic monitoring programs are now providing a wealth of detail about the structure and size of the broad-line region (BLR) in active galactic nuclei (AGNs) and on the nature of the continuum and its relationship to the emission lines (see Peterson 1993 for a review). The bright Seyfert 1 galaxy NGC 5548 is one of the sources that has received considerable attention in these efforts. Beginning in late 1988, the ultraviolet spectrum of this source was observed once every 4 days for an 8 month period with the *International Ultraviolet Explorer* (Clavel et al. 1991; hereafter Paper I). A concurrent ground-based campaign to monitor the variability of the optical spectrum was also carried out (Peterson et al. 1991, 1992; Dietrich et al. 1993; hereafter Papers II–IV, respectively). By combining the UV and optical results, it has also been possible to study the variability of the "small blue bump," a blend of ultraviolet Fe II and Balmer continuum emission (Maoz et al. 1993). More recently, the southern hemisphere Seyfert 1 galaxy NGC 3783 has been the subject of a similar monitoring effort (Reichert et al. 1994; Stirpe et al. 1994; hereafter Papers V and VI, respectively).

Since the completion of the original monitoring campaign in 1988–89, high temporal resolution, coordinated ground-based monitoring of NGC 5548 has been sustained. The results of the second year of the program are described in Paper III. The primary reasons for continuation of the program are (1) to examine the evolution of the emission-line profiles which

[1] Department of Astronomy, Ohio State University, 174 West 18th Avenue, Columbus, OH 43210.
[2] Harvard-Smithsonian Center for Astrophysics, 60 Garden Street, Cambridge, MA 02138.
[3] Mailing address: Lowell Observatory, Mars Hill Road, 1400 West, Flagstaff, AZ 86001.
[4] Sternberg Astronomical Institute, University of Moscow, Universitetskij prosp. 13, Moscow V-234, Russia.
[5] Dominion Astrophysical Observatory, 5071 West Saanich Road, Victoria, B.C., Canada, V8X 4M6.
[6] McDonald Observatory and Department of Astronomy, University of Texas, RLM 15.308, Austin, TX 78712.
[7] Department of Physics and Astronomy, University of Calgary, 2500 University Drive NW, Calgary, AB, Canada, T2N 1N4.
[8] Crimean Astrophysical Observatory, P/O Nauchny, 334413 Crimea, Ukraine.
[9] Center for Astrophysics and Space Sciences, University of California at San Diego, C-011, La Jolla, CA 92093.
[10] Universitäts-Sternwarte Göttingen, Geismarlandstrasse 11, D-37083 Göttingen, Germany.
[11] Department of Astronomy, University of California, Berkeley, CA 94720.
[12] Multiple Mirror Telescope Observatory, University of Arizona, Tucson, AZ 85721.
[13] Deceased.
[14] Space Telescope Science Institute, 3700 San Martin Drive, Baltimore, MD 21218.
[15] Mailing address: Sterrekundig Instituut, University of Utrecht, P.O. Box 80000, NL-3508 TA, Utrecht, The Netherlands.
[16] Observatories of the Carnegie Institution of Washington, 813 Santa Barbara Street, Pasadena, CA 91101.
[17] Department of Astronomy, University of California, Math-Science Building, Los Angeles, CA 90024.
[18] Osservatorio Astronomico di Bologna, Via Zamboni 33, I-40126, Bologna, Italy.
[19] Institute of Astronomy, Madingley Road, Cambridge CB3 0HZ, United Kingdom.
[20] Royal Greenwich Observatory, Madingley Road, Cambridge CB3 0EZ, United Kingdom.
[21] Department of Mathematics, Physics, and Engineering, Mount Royal College, Calgary, Canada, T3E 6K6.
[22] Special Astrophysical Observatory, Russian Academy of Sciences, Nizhni Arkhys, Stavropolsky Kraj, 357140, Russia.
[23] Mailing address: Steward Observatory, University of Arizona, Tucson, AZ 85721.
[24] Departamento de Astronomia, Instituto de Física, Universidade Federal do Rio Grande do Sul, Avenida Bento Gonçalves, 9500, CP15051, CEP 91500, Porto Alegre, RS, Brazil.

appear to change on timescales longer than the BLR light-crossing time (and thus probably are not attributable to excitation inhomogeneities in the BLR) and may be due to structural changes in the BLR on the dynamical timescales of a few years, and (2) to study the continuum variability at high temporal resolution in order to determine its short timescale behavior over long time intervals.

In this contribution, we present the first results obtained by doubling the temporal baseline of the published data to 4 yr. We present optical continuum and Hβ emission-line fluxes determined from spectra obtained between 1990 December and 1992 October. The observations are described in § 2, and in § 3 we outline the procedure by which we produce a homogeneous set of continuum and emission-line flux measurments. The results of some preliminary time-series analyses are described in § 4, and our results are summarized in § 5.

2. OBSERVATIONS

A complete log of spectroscopic observations appears in Table 1. Columns (1) and (2) give the UT date and Julian date, respectively, of each observation. Column (3) gives a code which indicates the observatory and instrument used to obtain the spectrum; these codes are the same as in Papers II, III, and IV of this series. The projected spectrograph entrance aperture, in arcseconds, is given in column (4). The first dimension is the slit width in the dispersion direction, and the second dimension is the slit length in the cross-dispersion direction; in the case of CCDs, the second entry is the "extraction window" used. The slit position angle is given in column (5), measured in the conventional manner, eastward from north; the cross-dispersion direction runs north–south for a position angle 0°. An estimate of the seeing, when it was recorded at the telescope, is given in column (6). The nominal spectral resolution is given in column (7), and column (8) contains the approximate wavelength range covered by the data. Finally, to aid future investigators who will make use of these data, column (9) gives a unique identifier by which the spectrum is known to the IRAF reduction system, and which is contained in the FITS file header. The file naming convention is the same as used in Papers II and III: the first two characters ("n5") identify the galaxy as NGC 5548, and the next four characters (e.g., "8225") contain the four least significant figures in the Julian date, as in column (2). The next character gives the observatory code, as in column (3). When necessary, an additional arbitrary character is added to eliminate any remaining ambiguity.

3. ANALYSIS OF THE DATA

As in Papers II and III, we will at this time restrict our attention only to those spectra in Table 1 which cover the Hβ spectral region, and discuss only the variability of the optical continuum and the Hβ emission-line fluxes. Further analysis, including discussion of the emission-line profile variability, will be left to future papers.

3.1. *Absolute Calibration of the Spectra*

As is usual in AGN emission-line studies based on optical spectrophotometry, flux calibration has been carried out by assuming that the narrow emission lines are constant in flux throughout the duration of the monitoring program. The light travel time and recombination time for the extended narrow-line region are both sufficiently long that this is almost certainly a valid assumption. In principle, all of the spectra can be placed on a common flux scale by multiplying each spectrum by a constant which is chosen to give the correct integrated flux in the narrow emission lines. The [O III] λ5007 line is especially useful for flux calibration of spectra of the Hβ region as it is strong and usually not strongly contaminated by other spectral features. The spectra can be placed on an absolute flux scale if the absolute flux of [O III] λ5007 is known. In Paper II, we obtained the absolute flux in the [O III] λ5007 line by averaging measurements made through large spectrograph entrance apertures on nights which were reported to be photometric by the observers. In Paper III, we repeated this analysis to ensure that our assumption of constant [O III] λ5007 flux is valid. We have again performed this check for the new data reported here. The [O III] λ5007 flux, transformed to the rest frame of NGC 5548 ($z = 0.0174$), is given in Table 2 for those spectra from Table 1 which were obtained through large apertures on photometric nights. These data are in excellent agreement with the measurements for the first 2 yr of the program, as given in Papers II and III. We continue to use the absolute flux given in Paper II (5.58×10^{-13} ergs s^{-1} cm^{-2}) in order to keep all of the measurements for all 4 yr on the same flux scale.

3.2. *Spectral Measurements*

Continuum (at 5100 Å in the rest frame of NGC 5548) and Hβ emission-line measurements were made from the spectra listed in Table 1 as described in Papers II and III. Data with a common origin, as designated by the individual codes in column (3) of Table 1, are assumed to be homogeneous, except in a few cases where significantly different spectrograph entrance apertures were employed. The flux ratios F_λ(5100 Å)/F([O III] λ5007) and F(Hβ)/F([O III] λ5007) were measured for each of the spectra in Table 1 in which these features appear. These measured flux ratios are given in Table 3, grouped by individual homgeneous data set. The continuum and Hβ fluxes can be placed on an absolute scale by multiplying each ratio by the adopted [O III] λ5007 flux, i.e., $F_{5007} = 5.58 \times 10^{-13}$ ergs s^{-1} cm^{-2}.

3.3. *Intercalibration of the Data*

The larger data sets in Table 3 reveal similar patterns of variability in both the continuum and the Hβ emission line. However, the light curves produced from the individual sets are slightly offset in flux from one another, and this is attributed to aperture effects. Following Papers II, III, and VI, we can determine an empirical correction for each of the data sets to bring them on to a common flux scale. This is done by adopting one of the larger data sets as a standard, and applying corrections to the other sets that bring measurements from the two sets that are closely spaced in time into agreement. We first define a point-source correction factor φ by the equation

$$F(\mathrm{H}\beta) = \varphi F_{5007}\left[\frac{F(\mathrm{H}\beta)}{F([\mathrm{O\ III}]\ \lambda5007)}\right]_{\mathrm{obs}}, \qquad (1)$$

where F_{5007} is the absolute [O III] λ5007 flux, and the observed ratio is as given in Table 3. This factor accounts for the fact that different apertures result in different amounts of light loss for the point-spread function (which describes the surface-brightness distribution of both the broad lines and the AGN continuum source) and the partially extended narrow-line region. We note, of course, that this correction factor is in fact a function of seeing. We do not attempt to correct for seeing effects, and this is probably our largest single source of uncertainty. If the surface brightness distribution of the

TABLE 1

LOG OF SPECTROSCOPIC OBSERVATIONS

UT Date (1)	Julian Date (2,440,000+) (2)	Code (3)	Aperture Size (4)	Aperture P.A. (5)	Seeing (″) (6)	Resolution (Å) (7)	Range (Å) (8)	IRAF File (9)
1990 Nov 29	8225	D	4.0 × 9.0	114	1.5–2	8	3450–9920	n58225d
1990 Dec 5	8231	A	5.0 × 7.6	90	3	9	4550–5680	n58231a
1990 Dec 11	8236	A	5.0 × 7.6	90	3	9	4530–5670	n58236a
1990 Dec 27	8252	A	5.0 × 7.6	90	3	9	4600–5680	n58252a
1991 Jan 6	8262	H	4.0 × 10.0	140	1–1.5	20	3880–7030	n58262h
1991 Jan 11	8267	A	5.0 × 7.6	90	4	9	4600–5670	n58267a
1991 Jan 19	8275	A	5.0 × 7.6	90	3	9	4600–5650	n58275a
1991 Jan 24	8280	A	5.0 × 7.6	90	3	9	4520–5670	n58280a
1991 Jan 31	8287	A	5.0 × 7.6	90	2	9	4530–5670	n58287a
1991 Feb 7	8294	A	5.0 × 7.6	90	3	9	4520–5660	n58294a
1991 Feb 11	8298	F	3.2 × 6.4	90	...	5	4660–7060	n58298f
1991 Feb 14	8301	N	8.8 × 12.0	0	...	12	4590–7230	n58301n
1991 Feb 14	8302	F	3.2 × 6.4	90	...	5	4660–7060	n58302f
1991 Feb 23	8310	A	5.0 × 7.6	90	1.5	9	4520–5660	n58310a
1991 Mar 8	8323	A	5.0 × 7.6	90	3	9	4530–5670	n58323a
1991 Mar 8	8323	F	3.2 × 6.4	90	...	5	4660–7060	n58323f
1991 Mar 9	8324	F	3.2 × 6.4	90	...	5	4660–7060	n58324f
1991 Mar 10	8325	F	3.2 × 6.4	90	...	5	4660–7060	n58325f
1991 Mar 14	8329	F	3.2 × 6.4	90	...	5	4660–7060	n58329f
1991 Mar 15	8330	F	3.2 × 6.4	90	...	5	4660–7060	n58330f
1991 Mar 23	8338	A	5.0 × 7.6	90	2.5	9	4530–5670	n58338a
1991 Mar 26	8341	L	2.0 round	...	4	3	4100–5140	n58341l
1991 Mar 29	8344	A	5.0 × 7.6	90	4	9	4500–5640	n58344a
1991 Apr 5	8351	A	5.0 × 7.6	90	3	9	4510–5650	n58351a
1991 Apr 6	8352	A	5.0 × 7.6	90	3	9	4520–5650	n58352a
1991 Apr 7	8353	F	3.2 × 6.4	90	...	5	4610–7060	n58353f
1991 Apr 7	8354	H	4.0 × 10.0	60	2	20	3910–6980	n58354h
1991 Apr 8	8354	F	3.2 × 6.4	90	...	5	4610–7060	n58354f
1991 Apr 9	8355	F	3.2 × 6.4	90	...	5	4660–7060	n58355f
1991 Apr 10	8356	F	3.2 × 6.4	90	...	5	4720–7060	n58356f
1991 Apr 14	8360	F	3.2 × 6.4	90	...	5	4610–7060	n58360f
1991 Apr 15	8361	F	3.2 × 6.4	90	...	5	4610–7060	n58361f
1991 Apr 16	8362	F	3.2 × 6.4	90	...	5	4660–7060	n58362f
1991 Apr 19	8365	L	2.0 round	...	4	3	4070–5100	n58365l
1991 Apr 19	8365	A	5.0 × 7.6	90	2	9	4520–5660	n58365a
1991 Apr 19	8366	H	4.0 × 10.0	61	2	20	3900–7000	n58366h
1991 May 2	8378	A	5.0 × 7.6	90	2	9	4530–5670	n58378a
1991 May 5	8381	H	4.0 × 10.0	241	1.3	20	3910–7000	n58381h
1991 May 8	8384	F	3.2 × 6.4	90	...	5	4590–7060	n58384f
1991 May 10	8386	A	5.0 × 7.6	90	4	9	4520–5660	n58386a
1991 May 17	8393	A	5.0 × 7.6	90	2.5	9	4520–5660	n58393a
1991 May 18	8394	F	3.2 × 6.4	90	...	5	4580–7060	n58394f
1991 May 19	8395	F	3.2 × 6.4	90	...	5	4610–7060	n58395f
1991 May 20	8396	L	2.0 round	...	3	3	4060–5100	n58396l
1991 May 24	8400	A	5.0 × 7.6	90	1.5	9	4540–5660	n58400a
1991 Jun 7	8414	A	5.0 × 7.6	90	3	9	4530–5670	n58414a
1991 Jun 8	8415	F	3.2 × 6.4	90	...	5	4510–7060	n58415f
1991 Jun 14	8421	A	5.0 × 7.6	90	2	9	4470–5610	n58421a
1991 Jun 16	8423	V	1.2 × 10.0	...	...	16	3200–7980	n58423v
1991 Jun 20	8427	V	1.2 × 10.0	...	...	9	3500–5970	n58427v
1991 Jun 21	8428	V	1.2 × 5.0	...	...	16	3650–8600	n58428v
1991 Jun 21	8428	H	8.0 × 7.9	60.1	1.5	8	4270–7300	n58428ha
1991 Jun 21	8428	H	2.0 × 8.6	60.1	1.5	4	4540–5330	n58428hb
1991 Jun 21	8428	H	2.0 × 7.9	60.1	1.5	8	6080–7220	n58428hc
1991 Jun 24	8431	A	5.0 × 7.6	90	2	9	4530–5670	n58431a
1991 Jul 18	8455	A	5.0 × 7.6	90	2	9	4520–5650	n58455a
1991 Jul 19	8456	A	5.0 × 7.6	90	3	9	4520–5660	n58456a
1991 Jul 20	8457	H	4.0 × 10.0	58	2	20	3910–6980	n58457h
1991 Jul 23	8460	A	5.0 × 7.6	90	3	9	4520–5660	n58460a
1991 Aug 5	8473	H	4.0 × 10.0	61	4	20	3910–7040	n58473h
1991 Aug 5	8474	M	2.0 × 10.0	90	1.5	9	3950–8100	n58474m
1991 Aug 8	8477	M	2.0 × 10.0	90	2	3	4070–5560	n58477m
1991 Aug 10	8479	M	2.0 × 10.0	90	2	4	5510–7640	n58479n
1991 Aug 20	8488	H	4.0 × 10.0	61	1.5	20	3910–7060	n58488h
1991 Sep 7	8507	M	1.0 × 10.0	0	1.5	20	4340–5550	n58507ma
1991 Sep 7	8507	M	1.0 × 10.0	0	1.5	15	5670–7380	n58507mb
1991 Sep 13	8512	A	5.0 × 7.6	90	2	9	4560–5660	n58512a
1991 Sep 14	8513	A	5.0 × 7.6	90	2	9	4550–5650	n58513a
1991 Sep 15	8514	A	5.0 × 7.6	90	1.5–2	9	4550–5650	n58514a

TABLE 1—*Continued*

UT Date (1)	Julian Date (2,440,000+) (2)	Code (3)	Aperture Size (4)	Aperture P.A. (5)	Seeing (″) (6)	Resolution (Å) (7)	Range (Å) (8)	IRAF File (9)
1991 Sep 16	8515	H	4.0 × 10.0	60	1–1.5	20	3140–7080	n58515h
1991 Sep 17	8516	A	5.0 × 7.6	90	2.5	9	4560–5680	n58516a
1991 Oct 2	8531	H	4.0 × 10.0	60	1	20	3240–7500	n58531h
1991 Oct 5	8534	A	5.0 × 7.6	90	1.5	9	4540–5640	n58534a
1992 Jan 1	8623	H	4.0 × 10.0	123	1.5–2	20	3960–7100	n58623h
1992 Jan 9	8630	W	2.0 × 10.0	90	2	7	6050–7160	n58630w
1992 Jan 9	8630	H	4.0 × 10.0	123	1.5–2	8	3900–7070	n58630h
1992 Jan 10	8631	W	2.0 × 10.0	90	2	9	5970–7080	n58631w
1992 Jan 15	8636	A	5.0 × 7.5	90	...	10	4470–5650	n58636a
1992 Jan 23	8644	A	5.0 × 7.5	90	3	10	4530–5700	n58644a
1992 Jan 30	8651	A	5.0 × 7.5	90	...	10	4530–5700	n58651a
1992 Feb 3	8655	R	3.0 × 15.0	0	...	8	4550–7070	n58655r
1992 Feb 9	8662	F	3.2 × 6.4	90	...	5	4610–7170	n58662f
1992 Feb 18	8670	A	5.0 × 7.5	90	...	10	4600–5700	n58670a
1992 Feb 24	8676	A	5.0 × 7.5	90	4–5	10	4500–5650	n58676a
1992 Feb 25	8677	X	5.0 × 12.0	...	...	5	3660–7200	n58677x
1992 Feb 26	8679	F	3.2 × 6.4	90	...	5	4660–7200	n58679f
1992 Feb 28	8681	F	3.2 × 6.4	90	...	5	4660–7220	n58681f
1992 Feb 29	8682	F	3.2 × 6.4	90	...	5	4660–7200	n58682f
1992 Mar 6	8687	F	3.2 × 6.4	90	...	5	4660–7200	n58687f
1992 Mar 7	8688	F	3.2 × 6.4	90	...	5	4660–7200	n58689f
1992 Mar 10	8691	A	5.0 × 7.5	90	2–3	10	4550–5700	n58691a
1992 Mar 11	8692	J	5.0 × 12.0	90	2–3	8	3160–5780	n58692j
1992 Mar 11	8693	F	3.2 × 6.4	90	...	5	4660–7240	n58693f
1992 Mar 13	8695	H	4.0 × 10.0	59	3–5	20	3300–9990	n58695h
1992 Mar 18	8699	A	5.0 × 7.5	90	2–3	10	4500–5650	n58699a
1992 Mar 26	8707	F	3.2 × 6.4	90	...	5	4660–7170	n58707f
1992 Apr 1	8713	A	5.0 × 7.5	90	3–4	10	4500–5650	n58713a
1992 Apr 5	8718	W	2.0 × 10.0	90	1.5	6	4340–5530	n58718wa
1992 Apr 6	8718	W	2.0 × 10.0	90	2	9	6020–7140	n58718wb
1992 Apr 8	8720	A	5.0 × 7.5	90	1.5	10	4570–5650	n58720a
1992 Apr 14	8726	A	5.0 × 7.5	90	...	10	4530–5680	n58726a
1992 Apr 21	8733	A	5.0 × 7.5	90	3–3	10	4530–5680	n58733a
1992 Apr 21	8733	H	4.0 × 10.0	62	2–3	8	3090–10000	n58733h
1992 Apr 22	8734	D	1.0 × 10.0	53	2	5	3170–9390	n58734d
1992 Apr 24	8736	F	3.2 × 6.4	90	...	5	4660–7170	n58736f
1992 Apr 25	8737	F	3.2 × 6.4	90	...	5	4660–7170	n58737f
1992 Apr 29	8742	W	2.3 × 10.0	90	3.5	7	4300–5490	n58742w
1992 Apr 30	8742	A	5.0 × 7.5	90	3	10	4510–5670	n58742a
1992 May 1	8743	W	2.0 × 10.0	90	3	6	4320–5510	n58743wa
1992 May 1	8743	W	2.0 × 10.0	90	3	7	6000–7120	n58743wb
1992 May 1	8743	F	3.2 × 6.4	90	...	5	4660–7170	n58743f
1992 May 1	8744	W	2.3 × 10.0	90	2.5–4	7	4330–5480	n58744wa
1992 May 1	8744	W	2.3 × 10.0	90	4	7	5950–7080	n58744wb
1992 May 2	8744	F	3.2 × 6.4	90	...	5	4660–7170	n58744f
1992 May 2	8745	W	2.3 × 10.0	90	2.5	7	4290–5480	n58745wa
1992 May 2	8745	W	2.3 × 10.0	90	2.5	9	5980–7110	n58745wb
1992 May 3	8745	F	3.2 × 6.4	90	...	5	4660–7170	n58745f
1992 May 3	8746	W	2.3 × 10.0	90	2	6	4290–5470	n58746wa
1992 May 4	8746	W	2.3 × 10.0	90	2	7	5950–7080	n58746wb
1992 May 5	8747	E	5.0 × 14.5	90	...	5	4660–5290	n58747e
1992 May 6	8748	F	3.2 × 6.4	90	...	5	4660–7160	n58748f
1992 May 8	8750	A	5.0 × 7.5	90	2	10	4520–5680	n58750a
1992 May 8	8750	F	3.2 × 6.4	90	...	5	4660–7170	n58750f
1992 May 23	8765	F	3.2 × 6.4	90	...	5	4580–7140	n58765f
1992 May 23	8765	H	4.0 × 10.0	62	1.5	8	3200–10200	n58765h
1992 May 24	8766	F	3.2 × 6.4	90	...	5	4580–7170	n58766f
1992 May 26	8769	R	3.0 × 15.0	0	...	15	4550–7030	n58769r
1992 May 27	8769	F	3.2 × 6.4	90	...	5	4580–7170	n58769f
1992 May 28	8771	W	2.3 × 10.0	90	2	6	4300–5490	n58771wa
1992 May 28	8771	W	2.3 × 10.0	90	2	7	5960–7080	n58771wb
1992 Jun 3	8776	E	5.0 × 10.6	90	...	8	4290–5230	n58776e
1992 Jun 3	8777	W	2.3 × 10.0	90	1.5	6	4290–5480	n58777wa
1992 Jun 3	8777	W	2.3 × 10.0	90	1.5	9	6050–7180	n58777wb
1992 Jun 4	8778	W	2.3 × 10.0	90	1.5	6	4220–5410	n58778w
1992 Jun 5	8778	F	3.2 × 6.4	90	...	5	4580–7150	n58778f
1992 Jun 6	8779	F	3.2 × 6.4	90	...	5	4580–7170	n58779f
1992 Jun 7	8780	A	5.0 × 7.5	90	1.5	10	4540–5700	n58780a
1992 Jun 7	8780	F	3.2 × 6.4	90	...	5	4580–7150	n58780f
1992 Jun 10	8783	H	4.0 × 10.0	61	1.5	8	3230–10200	n58783ha
1992 Jun 10	8783	H	4.0 × 10.0	61	1.5	4	5850–7290	n58783hb

TABLE 1—*Continued*

UT Date (1)	Julian Date (2,440,000+) (2)	Code (3)	Aperture Size (4)	Aperture P.A. (5)	Seeing (″) (6)	Resolution (Å) (7)	Range (Å) (8)	IRAF File (9)
1992 Jun 16	8739	A	5.0 × 7.5	90	1.5	10	4550–5710	n58789a
1992 Jun 19	8793	M	1.3 round	...	3	12	3820–7340	n58793m
1992 Jun 23	8796	A	5.0 × 7.5	90	3	10	4490–5650	n58796a
1992 Jun 26	8799	V	1.2 × 6.0	...	1	15	4150–9190	n58799v
1992 Jun 28	8801	F	3.2 × 6.4	90	...	5	4660–7200	n58801f
1992 Jun 30	8804	W	2.3 × 10.0	90	2.5	7	4250–5450	n58804w
1992 Jul 1	8804	A	5.0 × 7.5	90	2	10	4510–5680	n58804a
1992 Jul 2	8805	F	3.2 × 6.4	90	...	5	4660–7170	n58805f
1992 Jul 7	8810	E	5.0 × 11.8	90	...	8	4260–5210	n58810e
1992 Jul 7	8810	H	4.0 × 10.0	60	1.5	8	3230–10200	n58810ha
1992 Jul 7	8810	H	4.0 × 10.0	55	1.5	4	5860–7430	n58810hb
1992 Jul 8	8812	M	2.0 × 10.0	0	1.5	5	3680–5890	n58812ma
1992 Jul 8	8812	M	2.0 × 10.0	0	1.5	7	5490–9710	n58812mb
1992 Jul 10	8813	E	5.0 × 7.2	90	...	5	4740–5210	n58813e
1992 Jul 12	8816	M	2.0 × 10.0	0	1	5	3680–5890	n58816ma
1992 Jul 12	8816	M	2.0 × 10.0	0	1	7	5510–9260	n58816mb
1992 Jul 14	8817	A	5.0 × 7.5	90	3–4	10	4550–5720	n58817a
1992 Jul 15	8818	E	5.0 × 5.8	90	...	5	4690–5160	n58818e
1992 Jul 22	8825	A	5.0 × 7.5	90	1.5–2	10	4540–5710	n58825a
1992 Jul 26	8830	W	2.0 × 10.0	90	1	6	4430–5620	n58830wa
1992 Jul 26	8830	W	2.0 × 10.0	90	1	7	6050–7180	n58830wb
1992 Jul 27	8831	W	2.0 × 10.0	90	2	6	4320–5510	n58831w
1992 Jul 28	8831	A	5.0 × 7.5	90	...	10	4580–5750	n58831a
1992 Jul 29	8833	W	2.0 × 10.0	90	3	7	4350–5540	n58833wa
1992 Jul 29	8833	W	2.0 × 10.0	90	3	7	6120–7250	n58833wb
1992 Jul 30	8834	W	2.0 × 10.0	90	2.5	7	4300–5490	n58834wa
1992 Jul 30	8834	W	2.0 × 10.0	90	2.5	7	6090–7220	n58834wb
1992 Jul 31	8834	E	5.0 × 7.2	90	...	5	4710–5180	n58834e
1992 Jul 31	8835	W	2.0 × 10.0	90	1	7	4290–5480	n58835w
1992 Aug 1	8836	W	2.3 × 10.0	90	1.5	7	4240–5440	n58836wa
1992 Aug 1	8836	W	2.3 × 10.0	90	1.5	8	5970–7100	n58836wb
1992 Aug 2	8837	W	2.3 × 10.0	90	1	6	4400–5590	n58837w
1992 Aug 3	8837	H	4.0 × 10.0	60	1.5	8	3260–10180	n58837h
1992 Aug 5	8839	A	5.0 × 7.5	90	1–2	10	4570–5740	n58839a
1992 Aug 14	8848	A	5.0 × 7.5	90	1–2	10	4510–5680	n58848a
1992 Aug 23	8858	W	1.5 × 10.0	90	1.5	6	4300–5500	n58858w
1992 Aug 24	8858	H	3.0 × 7.0	90	...	12	3320–5460	n58858h
1992 Aug 25	8860	M	2.0 × 10.0	0	1	10	3860–9180	n58860m
1992 Aug 26	8861	W	1.5 × 10.0	90	1	5	4340–5520	n58861w
1992 Aug 27	8862	W	1.5 × 10.0	90	1	6	4370–5560	n58862w
1992 Aug 28	8862	A	5.0 × 7.5	90	1–2	10	4560–5720	n58862a
1992 Aug 29	8864	M	2.0 × 10.0	0	2	10	3870–9170	n58864m
1992 Aug 31	8866	M	2.0 × 10.0	0	1	10	3860–9180	n58866m
1992 Sep 2	8867	H	4.0 × 10.0	62	1.5	8	3160–10250	n58867h
1992 Sep 4	8869	A	5.0 × 7.5	90	1–2	10	4530–5690	n58869a
1992 Sep 11	8876	A	5.0 × 7.5	90	2	10	4580–5730	n58876a
1992 Sep 18	8883	A	5.0 × 7.5	90	...	10	4540–5710	n58883a
1992 Sep 21	8886	H	4.0 × 10.0	61	1.5	8	3160–10250	n58886h
1992 Sep 24	8889	A	5.0 × 7.5	90	1.5	10	4500–5670	n58889a
1992 Oct 3	8898	A	5.0 × 7.5	90	2–3	10	4510–5670	n58898a
1992 Oct 3	8898	H	4.0 × 10.0	61	2	8	3200–10250	n58898h

Codes for Data Origin.—A: 1.8 m Perkins Telescope + Ohio State CCD Spectrograph; D: 5.0 m Hale Telescope + Double Spectrograph; E: 1.8 m DAO Telescope + CCD Spectrograph; F: 1.6 m Mount Hopkins Telescope + Reticon scanner; H: 3.0 m Shane Telescope + UV Schmidt Spectrograph (through 1992 Jan) + KAST Spectrograph (1992 March and after); J: 2.7 m McDonald Telescope + Cassegrain Grating Spectrograph; L: 6.0 m Special Astrophysical Observatory + TV scanner: M: 3.5 m and 2.2 m Calar Alto Observatory + CCD spectrographs; N: 1.0 m Nickel Telescope, Lick Observatory + CCD spectrograph; R: 1.5 m Loiano Telescope + CCD spectrograph; V: 4.5 m MMT + CCD spectrograph; W: 2.6 m Shajn Telescope, Crimean Astrophysical Observatory + CCD spectrograph; X: 1.0 m CTIO Telescope + 2D-Frutti.

narrow-line region is known, it is indeed possible to model a correction for seeing effects (e.g., Wanders et al. 1992), but there is no indication that such detailed modeling is necessary in the case of NGC 5548, at least for the larger apertures (see, however, Paper IV).

After correcting for aperture effects on the point-spread function to narrow-line ratio, another correction needs to be applied to adjust for the different amounts of starlight admitted by different apertures. An extended source correction G is thus defined as

$$F_\lambda(5100\ \text{Å}) = \varphi F_{5007}\left[\frac{F_\lambda(5100\ \text{Å})}{F([\text{O III}]\ \lambda 5007}\right]_{\text{obs}} - G\,. \qquad (2)$$

The process of intercalibrating the various data sets is then carried out by comparing pairs of nearly simultaneous obser-

TABLE 2

ABSOLUTE CALIBRATION CHECK

F([O III] λ5007) (10^{-13} ergs cm^{-2} s^{-1}) (1)	File Name (2)
5.32	n58275a
5.11	n58287a
5.30	n58393a
5.61	n58414a
5.61	n58473h
5.37	n58488h
5.41	n58515h
5.44	n58530h
5.51	n58623h
5.23	n58631h
5.32	n58765h
5.57	n58783ha
5.60	n58810ha
6.07	n58837h
5.33	n58898h
5.45 ± 0.23	Mean value from Years 3–4
5.48 ± 0.24	Mean value from Year 2
5.58 ± 0.27	Mean value from Year 1 (adopted absolute flux)

vations from different data sets to determine for each data set the values of the constants φ and G which are needed to adjust the emission-line and continuum fluxes to a common scale. Furthermore, the formal uncertainties in φ and G reflect the uncertainties in the individual data sets, so we can determine the nominal uncertainties for each data set if we assume that the errors added in quadrature. In practice, the interval which we define as "nearly simultaneous" is typically 2–4 days, which means that any real variability that occurs on timescales this short tends to be somewhat suppressed by the process that allows us to merge the different data sets.

As in Papers II and III, the data are calibrated relative to data set "A" because these data are fairly numerous, overlap reasonably well with most of the other data sets, and were obtained through a reasonably large aperture (5″.0 × 7″.6 for the first 3 yr, and 5″.0 × 7″.5 for the last year, with the very slight difference attributable to a detector change in autumn 1991). Fractional uncertainties of $\sigma_{\rm cont}/F_\lambda(5100\ \text{Å}) \approx 0.030$ and $\sigma_{\rm line}/F(H\beta) \approx 0.040$ for the continuum and Hβ line, respectively, are adopted for the similar, large-aperture, high-quality data sets "A" and "H," based on the differences between closely spaced observations within these sets. These values are very close to those found for the same sets in Papers II and III. The same uncertainties were adopted for the 5 m Palomar spectrum (set "D," large aperture), since these data were obtained in a way nearly identical to the Lick 3 m data (set "H"). The internal fractional errors of the set "F" data also have been determined from closely spaced observations (i.e., within 2 days), and found to be $\sigma_{\rm cont}/F_\lambda(5100\ \text{Å}) \approx 0.050$ and $\sigma_{\rm line}/F(\text{H}\beta) \approx 0.080$.

For the other data sets, it was possible to estimate the mean uncertainties in the measurements by comparing them to measurements from other sets for which the uncertainties are known and by assuming that the uncertainties for each set add in quadrature.

In Paper IV, it was shown that aperture effects are important for slit sizes smaller than $\sim$2″, and for this reason we have divided the Calar Alto data (set "M") into two separate sets, depending on whether a 1″ or a 2″ slit was employed.

The intercalibration constants we use for each data set are given in Table 4, and these constants are used with equations (1) and (2) to adjust the measurements given in Table 3 to a common flux scale, which corresponds to measurements through the 5″.0 × 7″.5 spectrograph entrance aperture used in set "A." The resultant values of the continuum flux F_λ(5100 Å) and the line flux F(Hβ) are given in Table 5, which contains the final light curve produced by computing the variance-weighted average of all the adjusted measurements obtained on a given Julian data.

We can perform a final check of our uncertainty estimates by examining the ratios of all pairs of observations in Table 5 which are separated by 2 days or less. There are 98 independent pairs of measurements within 2 days of one another. The dispersion about the mean (unity), divided by $2^{1/2}$, provides an estimate of the typical uncertainty in a single measurement. For the continuum, we find that the mean fractional error in a given measurement is 0.042. The average fractional uncertainty, from the quoted estimates for these same 98 measurements in Table 5, is 0.039, which implies that our error estimates are probably quite good. Examination of the Hβ emission-line fluxes indicates that the fractional uncertainty is 0.051, as compared to the mean of the quoted errors for these points, which is 0.056.

4. VARIABILITY ANALYSIS

4.1. *Characteristics of the Data Base*

Figure 1 shows the 5100 Å continuum and Hβ emission-line light curves from Table 5. These data span a total of 674 days, with an 89 day gap between the two observing seasons when NGC 5548 is too close to the Sun to observe. In Figure 2, the combined data from Table 5 and Papers II and III are shown. The entire data base covers 1390 days. The 89 day gap between

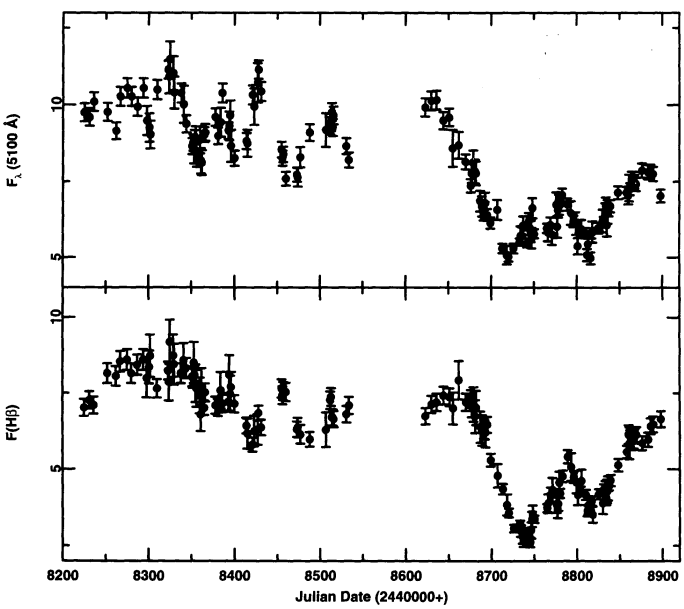

FIG. 1.—The continuum fluxes at 5100 Å (*top panel*) and Hβ emission-line fluxes (*bottom panel*) for NGC 5548, as given in Table 5, from 1990 December to 1992 October. Fluxes are in the rest frame of NGC 5548, and are in units of 10^{-15} ergs s^{-1} cm^{-2} Å^{-1} for the continuum and 10^{-13} ergs s^{-1} cm^{-2} for the line.

TABLE 3

MEASUREMENTS OF SPECTRA

Julian Date (2,440,000+) (1)	$100F_\lambda$(5100 Å) / F([O III] λ5007) (2)	F(Hβ) / F([O III] λ5007) (3)	IRAF File (4)	Julian Date (2,440,000+) (1)	$100F_\lambda$(5100 Å) / F([O III] λ5007) (2)	F(Hβ) / F([O III] λ5007) (3)	IRAF File (4)
A—Ohio State CCD							
8231.....	1.72	1.30	n58231a	8534.....	1.47	1.27	n58534a
8236.....	1.81	1.27	n58236a	8636.....	1.82	1.29	n58636a
8252.....	1.75	1.46	n58252a	8644.....	1.70	1.33	n58644a
8267.....	1.84	1.53	n58267a	8651.....	1.72	1.32	n58651a
8275.....	1.89	1.54	n58275a	8670.....	1.46	1.29	n58670a
8280.....	1.84	1.46	n58280a	8676.....	1.32	1.31	n58676a
8287.....	1.78	1.51	n58287a	8691.....	1.15	1.12	n58691a
8294.....	1.89	1.54	n58294a	8699.....	1.10	0.95	n58699a
8310.....	1.88	1.37	n58310a	8713.....	0.95	0.78	n58713a
8323.....	2.02	1.46	n58323a	8720.....	0.90	0.64	n58720a
8338.....	1.86	1.46	n58338a	8726.....	0.95	0.55	n58726a
8344.....	1.68	1.49	n58344a	8733.....	0.94	0.57	n58733a
8351.....	1.55	1.44	n58351a	8742.....	0.96	0.54	n58742a
8352.....	1.57	1.43	n58352a	8750.....	1.01	0.62	n58750a
8365.....	1.62	1.26	n58365a	8780.....	1.21	0.74	n58780a
8378.....	1.72	1.27	n58378a	8789.....	1.21	0.97	n58789a
8386.....	1.86	1.28	n58386a	8796.....	1.11	0.85	n58796a
8393.....	1.64	1.29	n58393a	8804.....	1.03	0.77	n58804a
8400.....	1.48	1.28	n58400a	8817.....	1.04	0.71	n58817a
8414.....	1.58	1.15	n58414a	8825.....	1.07	0.75	n58825a
8421.....	1.85	1.04	n58421a	8831.....	1.10	0.79	n58831a
8431.....	1.87	1.14	n58431a	8839.....	1.20	0.83	n58839a
8455.....	1.53	1.37	n58455a	8848.....	1.28	0.92	n58848a
8456.....	1.48	1.33	n58456a	8862.....	1.31	1.10	n58862a
8460.....	1.36	1.35	n58460a	8868.....	1.33	1.10	n58869a
8512.....	1.67	1.30	n58512a	8876.....	1.41	1.05	n58876a
8513.....	1.69	1.32	n58513a	8883.....	1.40	1.07	n58883a
8514.....	1.75	1.20	n58514a	8889.....	1.39	1.16	n58889a
8516.....	1.73	1.19	n58516a	8898.....	1.26	1.19	n58898a
D1—Palomar Double Spect. (Large Aperture)							
		8225.....	1.69	1.28	n58225d		
D2—Palomar Double Spect. (Small Aperture)							
		8734.....	0.66	0.70	n58734d		
E—DAO CCD							
8747.....	0.91	0.67	n58747e	8818.....	0.95	0.70	n58818e
8776.....	1.13	0.77	n58776e	8834.....	1.11	0.80	n58834e
8813.....	0.87	0.76	n58813e				
F—SAO Reticon							
8298.....	1.45	1.40	n58298f	8682.....	1.15	1.23	n58682f
8302.....	1.37	1.53	n58302f	8687.....	0.99	1.12	n58687f
8323.....	1.68	1.51	n58323f	8689.....	0.96	1.10	n58689f
8324.....	1.70	1.38	n58324f	8693.....	0.98	1.09	n58693f
8325.....	1.80	1.61	n58325f	8707.....	0.94	0.84	n58707f
8329.....	1.72	1.53	n58329f	8736.....	0.79	0.49	n58736f
8330.....	1.61	1.48	n58330f	8737.....	0.85	0.47	n58737f
8353.....	1.28	1.49	n58353f	8743.....	0.87	0.42	n58743f
8354.....	1.27	1.40	n58354f	8744.....	0.85	0.50	n58744f
8355.....	1.34	1.37	n58355f	8745.....	0.82	0.43	n58745f
8356.....	1.26	1.34	n58356f	8748.....	0.95	0.62	n58748f
8360.....	1.34	1.30	n58360f	8750.....	0.90	0.54	n58750f
8361.....	1.22	1.19	n58361f	8765.....	0.83	0.60	n58765f
8362.....	1.21	1.35	n58362f	8766.....	0.81	0.68	n58766f
8384.....	1.44	1.33	n58384f	8769.....	0.85	0.77	n58769f
8394.....	1.42	1.42	n58394f	8778.....	0.96	0.70	n58778f
8395.....	1.48	1.31	n58395f	8779.....	0.97	0.80	n58779f
8415.....	1.32	1.08	n58415f	8780.....	0.95	0.81	n58780f
8662.....	1.31	1.39	n58662f	8801.....	0.73	0.73	n58801f
8679.....	1.21	1.25	n58679f	8805.....	0.83	0.81	n58805f
8681.....	1.16	1.18	n58681f				

TABLE 3—*Continued*

Julian Date (2,440,000+) (1)	$100F_\lambda$(5100 Å) / F([O III] λ5007) (2)	$F(H\beta)$ / F([O III] λ5007) (3)	IRAF File (4)	Julian Date (2,440,000+) (1)	$100F_\lambda$(5100 Å) / F([O III] λ5007) (2)	$F(H\beta)$ / F([O III] λ5007) (3)	IRAF File (4)
H—Lick Shane CCD							
8262.....	1.58	1.47	n58262h	8630.....	1.76	1.30	n58630h
8354.....	1.58	1.48	n58354h	8695.....	1.08	1.18	n58695h
8366.....	1.57	1.37	n58366h	8733.....	0.98	0.60	n58733h
8381.....	1.55	1.28	n58381h	8765.....	1.00	0.70	n58765h
8428.....	1.96	1.26	n58428ha	8783.....	1.20	0.87	n58783ha
8457.....	1.44	1.38	n58457h	8810.....	0.97	0.76	n58810ha
8473.....	1.32	1.15	n58473h	8837.....	1.12	0.83	n58837h
8488.....	1.57	1.09	n58488h	8858.....	1.22	1.02	n58858h
8515.....	1.60	1.22	n58515h	8867.....	1.28	1.11	n58867h
8351.....	1.49	1.24	n58531h	8886.....	1.34	1.17	n58886h
8623.....	1.72	1.23	n58623h	8898.....	1.22	1.21	n58898h
J—McDonald 2.7 m CCD							
		8692.....	0.86	1.11	n58692j		
L—Special Astrophysical Observatory Scanner							
8341.....	1.57	1.65	n58341l	8396.....	1.31	1.48	n58396l
8365.....	1.37	1.33	n58365l				
M1—Calar Alto CCD (1″ aperture)							
8507.....	1.69	1.14	n58507ma	8793.....	1.20	0.92	n58793m
M2—Calar Alto CCD (2″ aperture)							
8474.....	1.25	1.17	n58474m	8860.....	1.14	1.13	n58860m
8477.....	1.37	1.13	n58477m	8864.....	1.23	1.09	n58864m
8812.....	0.78	0.67	n58812ma	8866.....	1.23	1.10	n58866m
8816.....	0.76	0.67	n58816ma				
N—Lick Nickel CCD							
		8301.....	2.72	1.35	n58301n		
R—Loiano CCD							
8655.....	1.50	1.36	n58655r	8769.....	1.02	0.78	n58769r
V—MMT CCD							
8423.....	1.37	1.13	n58423v	8428.....	1.53	1.19	n58428v
8427.....	1.51	1.14	n58427v	8799.....	0.68	0.83	n58799v
W—Crimean CCD							
8718.....	0.74	0.78	n58718wa	8830.....	0.97	0.79	n58830wa
8742.....	0.96	0.58	n58742w	8831.....	1.00	0.83	n58831w
8743.....	0.94	0.67	n58743wa	8833.....	1.01	0.86	n58833wa
8744.....	1.03	0.61	n58744wa	8834.....	1.08	0.84	n58834wa
8745.....	0.95	0.59	n58745wa	8835.....	0.94	0.87	n58835w
8746.....	0.90	0.61	n58746wa	8836.....	1.03	0.89	n58836wa
8771.....	0.88	0.88	n58771wa	8837.....	0.97	0.84	n58837w
8777.....	0.93	0.76	n58777wa	8858.....	1.14	1.11	n58858w
8778.....	1.01	0.76	n58778w	8861.....	1.19	1.19	n58861w
8804.....	0.97	0.85	n58804w	8862.....	1.14	1.17	n58862w
X—CTIO 2D-Frutti							
		8677.....	1.40	1.25	n58677x		

the third and fourth year is by far the largest gap in the coverage; the gaps between the first and second year and between the second and third year are only 52 days and 46 days, respectively. The general characteristics of the data base are summarized in Table 6.[25] The fractional variation F_{var} is the ratio of the rms fluctuation to the mean flux and is corrected for the effect of measurement errors (see Paper I). The parameter R_{max} is the ratio of maximum to minimum flux. Neither of these parameters has been adjusted for the effects of nonvarying components, such as the stellar continuum or the Hβ narrow line.

Inspection of Figure 2 shows that the character of the continuum variations was considerably different during the third

[25] The sampling characteristics given in Table 6 supersede the incorrect values given in Paper III.

TABLE 4

FLUX SCALE FACTORS

Data Set (1)	Point-Source Scale Factor φ (2)	Extended Source Correction G (10^{-15} ergs s^{-1} cm^{-2} Å^{-1}) (3)
A	1.000	0.000
D1	0.982	−0.491
D2	0.764 ± 0.075	−2.906 ± 0.347
E	0.900 ± 0.102	−1.075 ± 0.088
F	1.022 ± 0.085	−1.214 ± 0.497
H	0.982 ± 0.042	−0.491 ± 0.337
J	1.017 ± 0.018	−1.697 ± 0.197
L	0.932 ± 0.060	−1.846 ± 0.646
M1	0.989 ± 0.092	0.150 ± 0.395
M2	0.974 ± 0.060	−0.843 ± 0.381
N	1.109 ± 0.070	7.578 ± 0.322
R	0.922 ± 0.085	−0.869 ± 0.505
V	0.990 ± 0.067	−2.369 ± 0.479
W	0.882 ± 0.118	−1.439 ± 0.427
X	1.012 ± 0.043	0.132 ± 0.378

year (1991) of this program than it has been at other times. Compared to the other years in which NGC 5548 has been closely monitored, the continuum variations was more rapid and of lower amplitude. This behavior is reminiscent of that observed in NGC 3783 (Papers V and VI) and shows very clearly that the nature of the continuum variations can change over time.

The fourth year (1992) of this program is also notable in that NGC 5548 reached its faintest recorded state. This has also been reported by Iijima, Rafanelli, & Bianchini (1992). A sample spectrum obtained during this very low state is shown in Figure 3, along with a high-state spectrum from Paper I. The

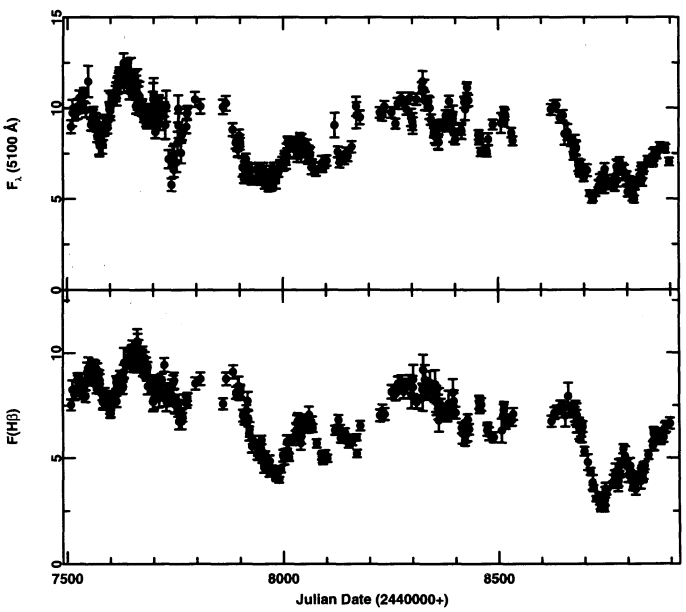

FIG. 2.—Optical continuum (5100 Å) and Hβ emission-line light curves are shown for all 4 yr of the NGC 5548 monitoring campaign. The data for the first year (1988 December–1989 October) and the second year (1989 December–1990 October) are from Tables A2 and 8, respectively, from Paper III, and the rest of the data are as in Table 5 and Fig. 1. Fluxes are in the rest frame of NGC 5548, and are in units of 10^{-15} ergs s^{-1} cm^{-2} Å^{-1} for the continuum and 10^{-13} ergs s^{-1} cm^{-2} for the line.

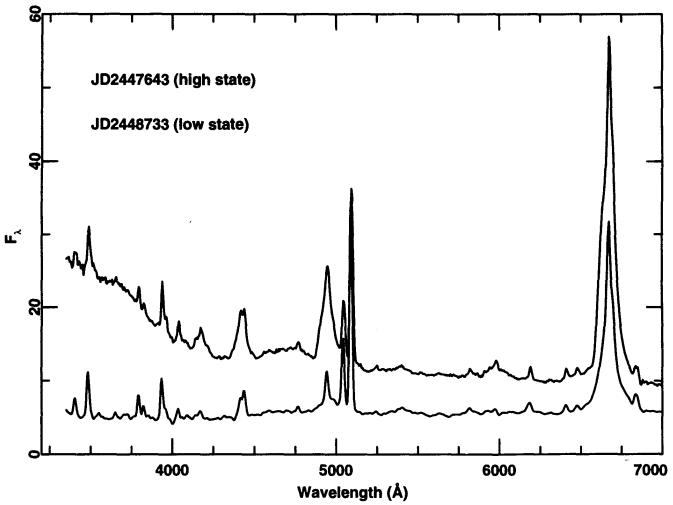

FIG. 3.—Two optical spectra, both obtained with the Lick 3 m Shane telescope, showing high and low states of NGC 5548. The lower spectrum was obtained on JD 2,448,733 (1992 May 1). The upper spectrum, from Paper I, was obtained on JD 2,447,643 (1989 April 27). Fluxes are in units of 10^{-15} ergs s^{-1} cm^{-2} Å^{-1} and are shown in the observed frame. The long wavelength end of the "small blue bump," which is prominent below 4100 Å in the high-state spectrum, is virtually absent in the low-state spectrum.

data obtained during this low state will be of particular use in determining both the narrow-line contributions to the broad emission features, and the starlight contribution to the optical spectra. This will be done in a future paper.

4.2. *Time-Series Analysis*

The lag between variations of the optical continuum and the Hβ emission-line response can be determined by cross correlation of the two light curves. Unfortunately, cross-correlation analysis of unevenly sampled series is not completely straightforward. Here we adjust for the irregular sampling by using two methods that are commonly employed in AGN variability studies, the interpolation method of Gaskell & Sparke (1986) and Gaskell & Peterson (1987), and the discrete correlation function (DCF) method of Edelson & Krolik (1988), in both cases with some minor modifications.

In the interpolation method, regular sampling is achieved by interpolating the light curves one at a time in a piecewise linear fashion between the real observations. The value of the cross-correlation function (CCF) is computed for any arbitrary lag τ by pairing each of the real data points in the emission-line light curve $L(t_i)$ with interpolated points in the continuum light curve $C(t_i - \tau)$ for all points which are within the real limits of each light curve. The CCF is then computed a second time, this time interpolating in the other series, pairing this time the real points $C(t_j)$ with the interpolated points $L(t_j + \tau)$. The results of these two computations are then averaged to form the final CCF. For the cross correlations performed here, we normalize the amplitude of the CCF at each lag by using the mean and variance computed only from those points which contribute to the CCF at that particular lag. This is in contrast to the usual practice of normalizing with the mean and variance for the whole time series (in other words, we are not assuming that the light curves are statistically stationary).

In the DCF method, problem of uneven sampling is dealt with by computing the correlation coefficient at lag τ using only real pairs of data separated by intervals in the range

TABLE 5

OPTICAL CONTINUUM AND Hβ LIGHT CURVES

Julian Date (2,440,000+) (1)	F_λ(5100 Å) (10^{-15} ergs s^{-1} cm^{-2} Å^{-1}) (2)	F(Hβ) (10^{-13} ergs s^{-1} cm^{-2}) (3)	Julian Date (2,440,000+) (1)	F_λ(5100 Å) (10^{-15} ergs s^{-1} cm^{-2} Å^{-1}) (2)	F(Hβ) (10^{-13} ergs s^{-1} cm^{-2}) (3)
8225.....	9.75 ± 0.29	7.01 ± 0.28	8651.....	9.60 ± 0.29	7.37 ± 0.29
8231.....	9.60 ± 0.29	7.25 ± 0.29	8655.....	8.59 ± 0.60	7.00 ± 0.52
8236.....	10.10 ± 0.30	7.09 ± 0.28	8662.....	8.69 ± 0.43	7.93 ± 0.63
8252.....	9.77 ± 0.29	8.15 ± 0.33	8670.....	8.15 ± 0.24	7.20 ± 0.29
8262.....	9.15 ± 0.27	8.06 ± 0.32	8676.....	7.37 ± 0.22	7.31 ± 0.29
8267.....	10.27 ± 0.31	8.54 ± 0.34	8677.....	7.77 ± 0.31	7.06 ± 0.35
8275.....	10.55 ± 0.32	8.59 ± 0.34	8679.....	8.11 ± 0.41	7.13 ± 0.57
8280.....	10.27 ± 0.31	8.15 ± 0.33	8681.....	7.83 ± 0.39	6.73 ± 0.54
8287.....	9.93 ± 0.30	8.43 ± 0.34	8682.....	7.77 ± 0.39	7.01 ± 0.56
8294.....	10.55 ± 0.32	8.59 ± 0.34	8687.....	6.86 ± 0.34	6.39 ± 0.51
8298.....	9.48 ± 0.47	7.98 ± 0.64	8689.....	6.69 ± 0.33	6.27 ± 0.50
8301.....	9.25 ± 0.46	8.35 ± 0.54	8691.....	6.42 ± 0.19	6.25 ± 0.25
8302.....	9.03 ± 0.45	8.73 ± 0.70	8692.....	6.58 ± 0.26	6.30 ± 0.31
8310.....	10.49 ± 0.31	7.64 ± 0.31	8693.....	6.80 ± 0.34	6.22 ± 0.50
8323.....	11.14 ± 0.29	8.23 ± 0.29	8695.....	6.41 ± 0.19	6.47 ± 0.26
8324.....	10.91 ± 0.55	7.87 ± 0.63	8699.....	6.14 ± 0.18	5.30 ± 0.21
8325.....	11.48 ± 0.57	9.18 ± 0.74	8707.....	6.57 ± 0.33	4.79 ± 0.38
8329.....	11.02 ± 0.55	8.73 ± 0.70	8713.....	5.30 ± 0.16	4.35 ± 0.17
8330.....	10.40 ± 0.52	8.44 ± 0.68	8718.....	5.08 ± 0.31	3.84 ± 0.34
8338.....	10.38 ± 0.31	8.15 ± 0.33	8720.....	5.02 ± 0.15	3.57 ± 0.14
8341.....	10.01 ± 0.60	8.58 ± 0.56	8726.....	5.30 ± 0.16	3.07 ± 0.12
8344.....	9.37 ± 0.28	8.31 ± 0.33	8733.....	5.52 ± 0.12	3.23 ± 0.09
8351.....	8.65 ± 0.26	8.03 ± 0.32	8734.....	5.72 ± 0.31	2.98 ± 0.19
8352.....	8.76 ± 0.26	7.98 ± 0.32	8736.....	5.72 ± 0.29	2.79 ± 0.22
8353.....	8.51 ± 0.43	8.50 ± 0.68	8737.....	6.06 ± 0.30	2.68 ± 0.21
8354.....	8.94 ± 0.23	8.08 ± 0.29	8742.....	5.49 ± 0.15	2.98 ± 0.11
8355.....	8.85 ± 0.44	7.81 ± 0.63	8743.....	6.13 ± 0.24	2.66 ± 0.16
8356.....	8.40 ± 0.42	7.64 ± 0.61	8744.....	6.23 ± 0.24	2.91 ± 0.17
8360.....	8.85 ± 0.44	7.41 ± 0.59	8745.....	5.98 ± 0.23	2.62 ± 0.16
8361.....	8.17 ± 0.41	6.79 ± 0.54	8746.....	5.87 ± 0.35	3.00 ± 0.27
8362.....	8.11 ± 0.41	7.70 ± 0.62	8747.....	5.64 ± 0.34	3.37 ± 0.25
8365.....	9.03 ± 0.24	7.00 ± 0.24	8748.....	6.63 ± 0.33	3.54 ± 0.28
8366.....	9.09 ± 0.27	7.51 ± 0.30	8750.....	5.79 ± 0.15	3.37 ± 0.12
8378.....	9.60 ± 0.29	7.09 ± 0.28	8765.....	5.96 ± 0.15	3.74 ± 0.13
8381.....	8.98 ± 0.27	7.01 ± 0.28	8766.....	5.83 ± 0.29	3.88 ± 0.31
8384.....	9.43 ± 0.47	7.58 ± 0.61	8769.....	6.08 ± 0.25	4.17 ± 0.23
8386.....	10.38 ± 0.31	7.14 ± 0.29	8771.....	5.77 ± 0.35	4.33 ± 0.39
8393.....	9.15 ± 0.28	7.20 ± 0.29	8776.....	6.75 ± 0.41	3.87 ± 0.29
8394.....	9.31 ± 0.47	8.10 ± 0.65	8777.....	6.02 ± 0.36	3.74 ± 0.34
8395.....	9.65 ± 0.48	7.47 ± 0.60	8778.....	6.57 ± 0.25	3.87 ± 0.23
8396.....	8.66 ± 0.52	7.70 ± 0.50	8779.....	6.75 ± 0.34	4.56 ± 0.37
8400.....	8.26 ± 0.25	7.14 ± 0.29	8780.....	6.72 ± 0.17	4.21 ± 0.15
8414.....	8.82 ± 0.26	6.42 ± 0.26	8783.....	7.07 ± 0.21	4.77 ± 0.19
8415.....	8.74 ± 0.44	6.16 ± 0.49	8789.....	6.75 ± 0.20	5.41 ± 0.22
8421.....	10.32 ± 0.31	5.80 ± 0.23	8793.....	6.47 ± 0.39	5.08 ± 0.46
8423.....	9.94 ± 0.60	6.24 ± 0.50	8796.....	6.19 ± 0.19	4.74 ± 0.19
8427.....	10.71 ± 0.64	6.30 ± 0.50	8799.....	6.13 ± 0.37	4.59 ± 0.37
8428.....	11.14 ± 0.30	6.83 ± 0.24	8801.....	5.38 ± 0.27	4.16 ± 0.33
8431.....	10.44 ± 0.31	6.36 ± 0.25	8804.....	5.83 ± 0.16	4.28 ± 0.16
8455.....	8.54 ± 0.26	7.64 ± 0.31	8805.....	5.95 ± 0.30	4.62 ± 0.37
8456.....	8.26 ± 0.25	7.42 ± 0.30	8810.....	5.81 ± 0.17	4.16 ± 0.17
8457.....	8.38 ± 0.25	7.56 ± 0.30	8812.....	5.08 ± 0.20	3.64 ± 0.18
8460.....	7.59 ± 0.23	7.53 ± 0.30	8813.....	5.44 ± 0.33	3.82 ± 0.29
8473.....	7.72 ± 0.23	6.30 ± 0.25	8816.....	4.97 ± 0.20	3.64 ± 0.18
8474.....	7.64 ± 0.31	6.36 ± 0.32	8817.....	5.80 ± 0.17	3.96 ± 0.16
8477.....	8.29 ± 0.33	6.14 ± 0.31	8818.....	5.85 ± 0.35	3.52 ± 0.26
8488.....	9.09 ± 0.27	5.97 ± 0.24	8825.....	5.97 ± 0.18	4.18 ± 0.17
8507.....	9.18 ± 0.55	6.29 ± 0.57	8830.....	6.21 ± 0.37	3.89 ± 0.35
8512.....	9.32 ± 0.28	7.25 ± 0.29	8831.....	6.18 ± 0.17	4.35 ± 0.16
8513.....	9.43 ± 0.28	7.37 ± 0.29	8833.....	6.41 ± 0.38	4.23 ± 0.38
8514.....	9.77 ± 0.29	6.70 ± 0.27	8834.....	6.70 ± 0.28	4.06 ± 0.23
8515.....	9.26 ± 0.28	6.68 ± 0.27	8835.....	6.07 ± 0.36	4.28 ± 0.38
8516.....	9.65 ± 0.29	6.64 ± 0.27	8836.....	6.51 ± 0.39	4.38 ± 0.39
8531.....	8.65 ± 0.26	6.79 ± 0.27	8837.....	6.54 ± 0.18	4.47 ± 0.16
8534.....	8.20 ± 0.25	7.09 ± 0.28	8839.....	6.70 ± 0.20	4.63 ± 0.19
8623.....	9.92 ± 0.30	6.74 ± 0.27	8848.....	7.14 ± 0.21	5.13 ± 0.20
8630.....	10.14 ± 0.30	7.12 ± 0.28	8858.....	7.15 ± 0.19	5.57 ± 0.20
8636.....	10.16 ± 0.31	7.20 ± 0.29	8860.....	7.04 ± 0.28	6.14 ± 0.31
8644.....	9.49 ± 0.28	7.42 ± 0.30	8861.....	7.30 ± 0.44	5.86 ± 0.53

TABLE 5—*Continued*

Julian Date (2,440,000+) (1)	F_λ(5100 Å) (10^{-15} ergs s^{-1} cm^{-2} Å^{-1}) (2)	F(Hβ) (10^{-13} ergs s^{-1} cm^{-2}) (3)	Julian Date (2,440,000+) (1)	F_λ(5100 Å) (10^{-15} ergs s^{-1} cm^{-2} Å^{-1}) (2)	F(Hβ) (10^{-13} ergs s^{-1} cm^{-2}) (3)
8862.....	7.25 ± 0.19	6.07 ± 0.22	8876.....	7.87 ± 0.24	5.86 ± 0.23
8864.....	7.53 ± 0.30	5.92 ± 0.30	8883.....	7.81 ± 0.23	5.97 ± 0.24
8866.....	7.53 ± 0.30	5.98 ± 0.30	8886.....	7.83 ± 0.23	6.41 ± 0.26
8867.....	7.50 ± 0.22	6.08 ± 0.24	8889.....	7.76 ± 0.23	6.47 ± 0.26
8869.....	7.42 ± 0.22	6.14 ± 0.25	8898.....	7.03 ± 0.21	6.64 ± 0.27

$\tau - \Delta t/2$ to $\tau + \Delta t/2$; the correlation function is thus binned into discrete time elements of width of Δt. The modifications we have introduced into the original formulation of Edelson & Krolik (1988) are (1) we do not weight the data points by their uncertainties, (2) we do not assume that the light curves are statistically stationary and we therefore normalize the correlation coefficient in each bin by using the mean and variance computed only from those data points in the bin, and (3) we do not adjust the variances by subtracting the uncertainties of the data points in quadrature (see Edelson & Krolik, eq. [3]).

A cross-correlation analysis has been performed for each of the 4 separate years as well as for the data set in its entirety. The upper panels of Figure 4 show the interpolation CCFs and DCFs for each of the 4 yr. The lower panels show both the corresponding continuum autocorrelation functions (ACF) and the sampling window ACFs; the latter are produced by averaging the ACFs obtained by repeatedly sampling a white-noise spectrum in exactly the same pattern as the real observations and then computing the ACF with the interpolation method. The interpolation process automatically introduces a correlation extending from zero lag to a value that characterizes the typical sampling interval, and thus the sampling window ACF provides a good indication of how much of the width of the ACF is introduced by the interpolation process rather than by real correlation of the continuum values at different times. The interpolation CCF, DCF, continuum ACF, and sampling window ACF for the entire 4 yr experiment are shown in Figure 5. The characteristics of the CCFs are summarized in Table 7. Here the parameter r_{max} is the peak value of the interpolation CCF, which occurs at a time delay Δt_{Peak}, and Δt_{Center} refers to the median of the half-maximum points. The uncertainties in these values are typically ~2–4 days. As before, we caution against ascribing much physical significance to any single number that is used to characterize the CCF, as interpolation of both the lag and its uncertainty depends on numerous factors, including the geometry of the BLR and on the continuum behavior (cf. Robinson & Pérez 1990). The relatively small uncertainty in the lag and the similarity of the solutions for the separate years shows that it is, however, a well-defined and experimentally repeatable quantity.

4.3. *The* Hβ *Transfer Function*

It is usually assumed that the relationship between the continuum light curve $C(t)$ and the emission-line light curve $L(t)$ can be written

$$L(t) = \int_{-\infty}^{\infty} \Psi(\tau) C(t - \tau) d\tau \,, \qquad (3)$$

where $\Psi(\tau)$ is the geometry-dependent transfer function (Blandford & McKee 1982). In principle, with the obervables $C(t)$ and $L(t)$, equation (3) can be inverted to solve for the transfer function. Transfer function solutions for NGC 5548, which have been obtained by employing a maximum entropy method (MEM), have been presented by Krolik et al. (1991) for the UV lines and by Horne, Welsh, & Peterson (1991) for Hβ. We have used the data described here and in Papers II and III to construct a MEM solution for the transfer function for

TABLE 6

VARIABILITY PARAMETERS AND SAMPLING CHARACTERISTICS

FEATURE (1)	NUMBER OF EPOCHS (2)	SAMPLING INTERVAL (days) Average (3)	SAMPLING INTERVAL (days) Median (4)	MEAN FLUX[a] (5)	F_{var} (6)	R_{max} (7)
		F_λ(5100 Å)				
Year 1 (1988 Dec–1989 Oct)	125	2.4	1	9.92	0.123	2.16
Year 2 (1989 Dec–1990 Oct)	94	3.4	2	7.25	0.133	1.83
Year 3 (1990 Nov–1991 Oct).....	65	4.8	3	9.40	0.094	1.51
Year 4 (1992 Jan–1992 Oct).....	83	3.4	2	6.72	0.169	2.04
Combined	367	3.8	2	8.42	0.210	2.51
		Hβ				
Year 1 (1988 Dec–1989 Oct)	132	2.3	1	8.62	0.095	1.57
Year 2 (1989 Dec–1990 Oct)	94	3.4	2	5.98	0.191	2.30
Year 3 (1990 Nov–1991 Oct).....	65	4.8	3	7.46	0.102	1.58
Year 4 (1992 Jan–1992 Oct).....	83	3.4	2	4.96	0.284	3.03
Combined	374	3.7	2	6.94	0.260	4.04

[a] Units as in Table 5.

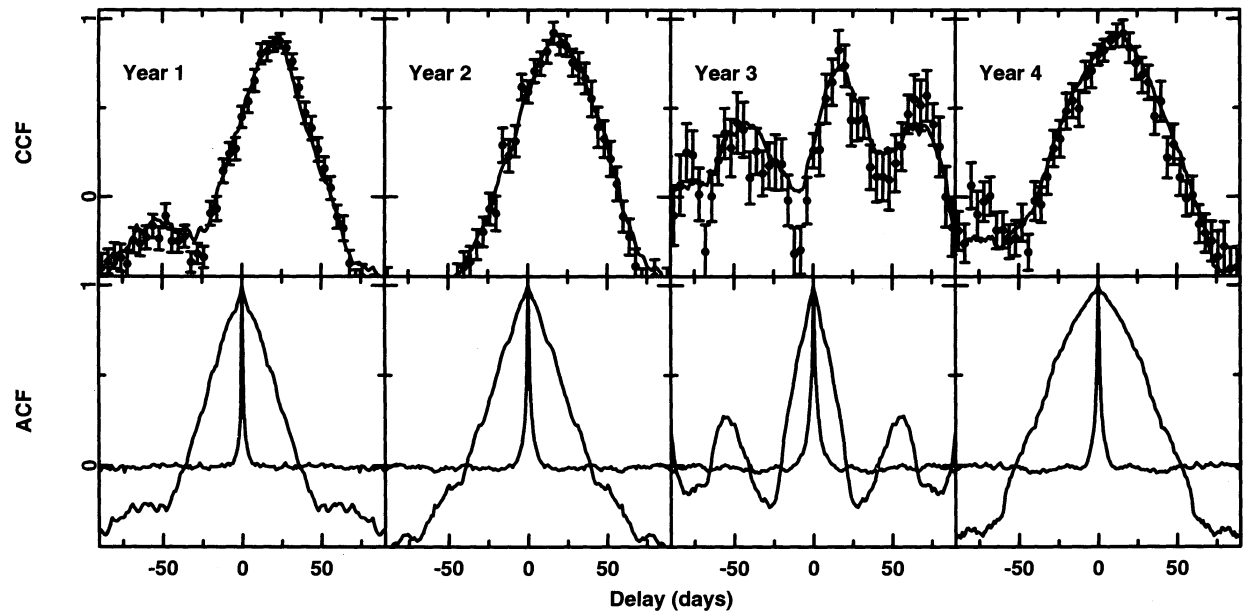

FIG. 4.—The cross-correlation functions for the optical continuum (5100 Å) and the Hβ emission line, for each of the 4 yr of this monitoring proram, are shown in the top row of panels. The interpolation CCF is shown as a smooth line, and the DCF values are plotted as individual points with associated uncertainties. The bin width for the DCF is 4 days. The corresponding continuum autocorrelation functions appear in the bottom row. Also illustrated in the bottom panels are the sampling window autocorrelations functions, which show the effect of interpolating the data between observations (Gaskell & Peterson 1987).

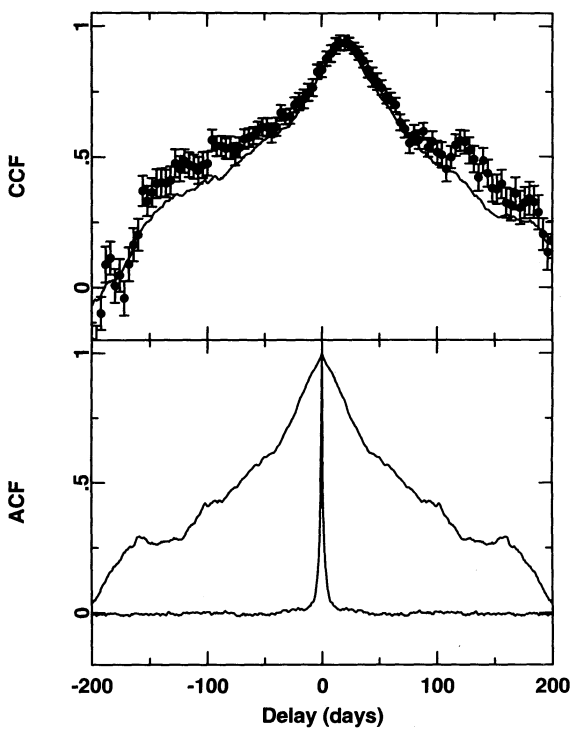

FIG. 5.—The top panel shows the optical continuum–Hβ cross-correlation function for the entire 4 yr monitoring program. The interpolation CCF is shown as a smooth line, and the DCF values are plotted as individual points with associated uncertainties. The bin width for the DCF is 4 days. The optical continuum autocorrelation function and the very narrow sampling window autocorrelation function appear in the lower panel.

each of the 4 yr separately and for the database as a whole. The details of the solution are discussed more completely by Peterson et al. (1993). The results of this analysis are shown in Figure 6. The transfer function for the total data set is quite similar to that derived from the first year's data alone and the expanded database appears to eliminate some of the structure at large lags that Horne et al. (1991) suspected was attributable to aliasing. However, the solutions for the separate years show some differences from year to year, particularly in year 4 (1992), when the peak response was more rapid than in previous years, as shown by the cross-correlation results (Table 7).

5. CONCLUSIONS

The optical spectroscopic monitoring program on the Seyfert 1 galaxy NGC 5548, described in Papers II and III, has been extended by 2 more years to provide a total baseline of nearly 1400 days. In this contribution, we have presented the first results from this extended campaign:

1. The Hβ emission-line variations follow those of the continuum on a timescale of about 18 days.
2. The continuum variations in NGC 5548 are usually rela-

TABLE 7

CROSS-CORRELATION RESULTS
OPTICAL CONTINUUM VS. Hβ

Data Set (1)	Δt_{Peak} (days) (2)	Δt_{Center} (days) (3)	r_{max} (4)
Year 1 (1988 Dec–1989 Oct)	22	19.4	0.87
Year 2 (1989 Dec–1990 Oct)	18	19.4	0.91
Year 3 (1990 Dec–1991 Oct)	18	18.5	0.74
Year 4 (1992 Jan–1992 Oct)	14	10.3	0.92
Combined	18	18.1	0.93

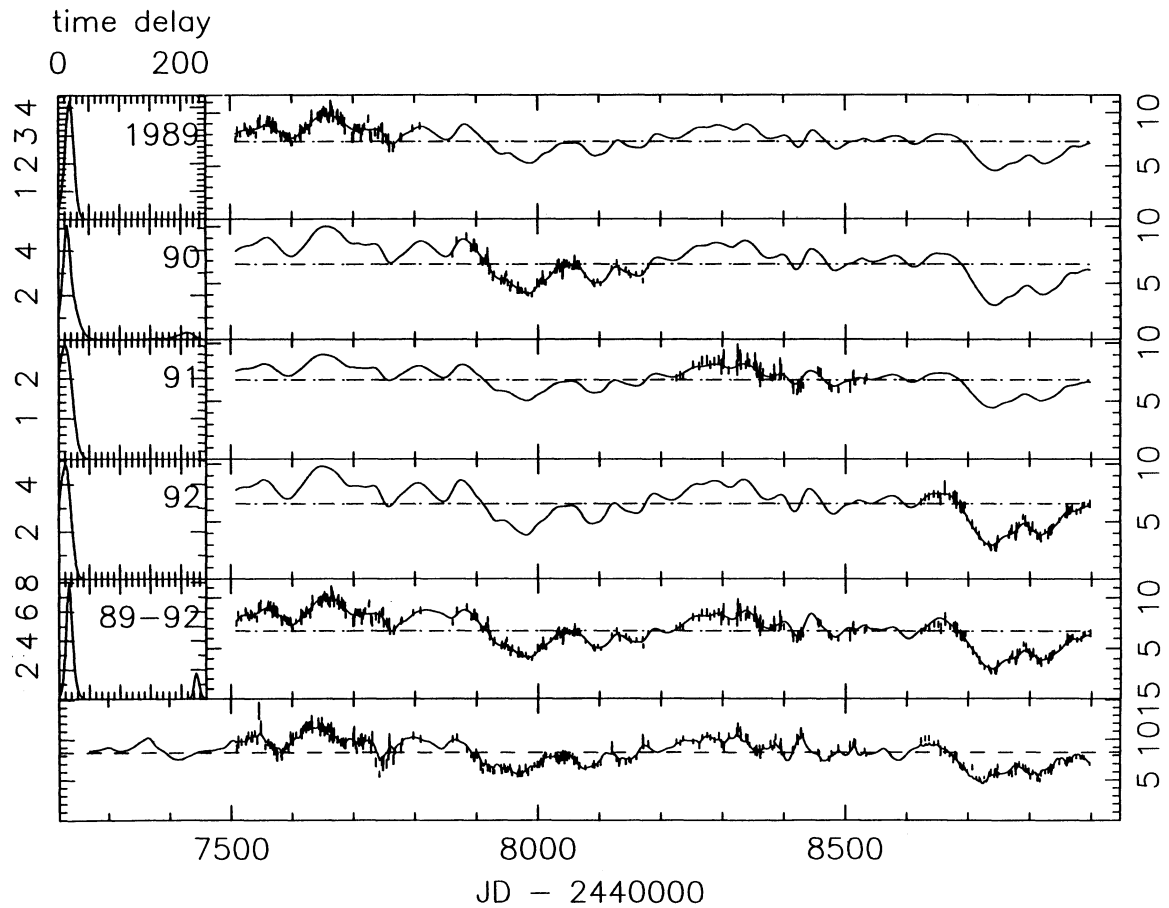

FIG. 6.—The Hβ transfer function for each of the 4 yr and for the entire 4 yr monitoring period. The bottom panel shows the maximum entropy fit to the observed continuum points, shown as vertical lines which correspond to 1 σ uncertainties. In the four upper panels, the transfer functions for the various subsets of the data (each individual year plus the entire data base) are shown on the left side and the right side of each panel shows the maximum entropy fit to the Hβ observations, also shown as 1 σ error bars. The dashed horizontal lines show the mean values of the light curves.

tively slow and well-resolved with the typical sampling of the experiment (2–4 days). However, during the third year the continuum variations were more rapid and of lower amplitude, similar to those observed in NGC 3783 in 1992, as described in Papers V and VI.

3. NGC 5548 went through an extremely faint state in 1992. The normally weak narrow components of the emission lines and stellar absorption features are relatively prominent in spectra obtained during this period and will be very useful in assessing how all of the data are affected by these nonvariable components.

4. The Hβ transfer function derived from the entire 4 yr database is similar to that obtained by Horne et al. (1991) for the first year's data. The transfer function is narrow and peaked at around 18 days with very low amplitude at zero lag. However, the transfer functions for the 4 separate years show some differences, notably that the peak response during the fourth year (1992) is at smaller time delays than in the previous years.

We are very grateful to the Directors and Telescope Allocation Committees of our various observatories for their support of this project. Individual investigators have benefitted from support from a number of agencies, including the following: the National Science Foundation: AST-9117086 (Ohio State University), AST-8714937 (University of Texas), AST-8957063 and AST-9003829 (University of California, Berkeley), and the NSF Graduate Fellowship program (T. M.); NASA: NAG5-1824 (Ohio State University), NAS8-30751 (Center for Astrophysics), and Long-Term Space Astrophysics grants NAGW-2678 (K. H.) and NAGW-3315 (B. M. P.); and BMFT grant Verbundforschung Astronomie DFG Ko857/13-1 (Universitäts-Sternwarte Göttingen). We thank the referee, D. Maoz, for helpful comments.

REFERENCES

Blandford, R. D., & McKee, C. F. 1982, ApJ, 255, 419
Clavel, J., et al. 1991, ApJ, 366, 64 (Paper I)
Dietrich, M., et al. 1993, ApJ, 408, 416 (Paper IV)
Edelson, R. A., & Krolik, J. H. 1988, ApJ, 333, 646
Gaskell, C. M., & Peterson, B. M. 1987, ApJS, 65, 1
Gaskell, C. M., & Sparke, L. S. 1986, ApJ, 305, 175
Horne, K., Welsh, W. F., & Peterson, B. M. 1991, ApJ, 367, L5
Iijima, T., Rafanelli, P., & Bianchini, A. 1992, A&A, 265, L25
Krolik, J. H., Horne, K., Kallman, T. R., Malkan, M. A., Edelson, R. A., & Kriss, G. A. 1991, ApJ, 371, 541
Maoz, D., et al. 1993, ApJ, 404, 576
Peterson, B. M. 1993, PASP, 105, 247
Peterson, B. M., et al. 1991, ApJ, 368, 119 (Paper II)
———. 1992, ApJ, 392, 470 (Paper III)
Peterson, B. M., Ali, B., Horne, K., Bertram, R., Lame, N. J., Pogge, R. W., & Wagner, R. M. 1993, ApJ, 402, 469
Reichert, G. A., et al. 1994, ApJ, 425, 582 (Paper V)
Robinson, A., & Pérez, E. 1990, MNRAS, 244, 138
Stirpe, G. M., et al. 1994, ApJ, 425, 609 (Paper VI)
Wanders, I., Peterson, B. M., Pogge, R. W., DeRobertis, M. M., & van Groningen, E. 1992, A&A, 266, 72